

# Synthesis and Photoluminescence of Spherical ZnS:Mn<sup>2+</sup> Particles

Bin Xia, I. Wuled Lenggoro, and Kikuo Okuyama\*

Department of Chemical Engineering, Graduate School of Engineering, Hiroshima University, Higashi-Hiroshima 739-8527, Japan

Received April 23, 2002. Revised Manuscript Received August 29, 2002

Spray pyrolysis, an aerosol decomposition technique, was first used to synthesize ZnS:Mn<sup>2+</sup> particles, and their optical properties were characterized. The effects of process parameters on the properties of ZnS:Mn<sup>2+</sup> particles were systematically investigated for Mn<sup>2+</sup> doping concentrations of 0–8 at. %. The results show that a number of parameters such as temperature, cationic source, doping concentration, solution composition, and concentration can affect particle morphology, crystalline phase, crystallinity, and thus the photoluminescence of the products. Micrometer/submicrometer particles have spherical shapes and dense microstructures. Excitation/emission bands and intensities are largely dependent on the synthesis temperature employed. The effects of different precursors on the product particles and photoluminescence were also investigated. Some of the phenomena observed differed from other reports. The mechanisms by which various process conditions affect particle morphology, crystalline phase, and luminescent property are discussed.

## Introduction

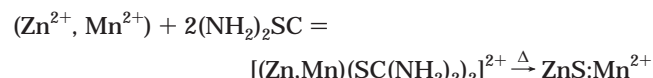
ZnS, an IIb–VI compound, is a promising host material for producing commercial phosphors. The cubic phase is stable at low temperature while the hexagonal phase is a high-temperature form.<sup>1</sup> Mn<sup>2+</sup>-doped ZnS (ZnS:Mn<sup>2+</sup>), which emits yellowish-orange under excitation, is one of the most important phosphors used in displays and is conventionally produced by a solid-state process at high temperatures (900–1200 °C) as bulk materials.<sup>1</sup> ZnS:Mn<sup>2+</sup> has been reported to show a quantum size effect when the crystal size is small enough (e.g., 3 nm), that is, the excitation shows blue shift and quantum efficiency is largely improved with decreasing crystalline size.<sup>2</sup> Recently, a number of techniques such as precipitation, microemulsion, sol–gel, chemical vapor deposition, and molecular beam epitaxy have been employed in the synthesis of ZnS:Mn<sup>2+</sup>.<sup>3–8</sup>

Aerosol decomposition, also referred to as spray pyrolysis, has been widely used in the synthesis of a variety of materials.<sup>9,10</sup> A precursor solution is atomized into aerosol droplets and then carried by a gas into a

hot reactor. After the droplets have been dried, the precursor is precipitated and thermally decomposed to form the desired product, which is then collected for characterization. Aerosol decomposition has been used to synthesize doped ZnS thin films by various cationic ions.<sup>11–13</sup> However, no studies on the synthesis and characterization of ZnS:Mn<sup>2+</sup> powders/particles have been reported using this technique. Due to the unique particle morphology and structures of the particles, we synthesized Mn<sup>2+</sup>-doped ZnS particles in a rapid (a few seconds) and continuous process in this work. Micrometer/submicrometer particles with spherical shapes and dense microstructures were produced. They were found to be composed of densely compacted nanometer crystals and their optical properties were characterized.

## Experimental Procedure

Three types of precursors, nitrates, chlorides, and acetates of Zn<sup>2+</sup> and Mn<sup>2+</sup>, were used as cationic sources. The same anionic sources of Zn<sup>2+</sup> and Mn<sup>2+</sup>, for example, Zn(NO<sub>3</sub>)<sub>2</sub> and Mn(NO<sub>3</sub>)<sub>2</sub>, were used to produce a ZnS:Mn<sup>2+</sup> sample. Thiourea (Tu) was employed as a sulfur source.<sup>14</sup> In an aqueous solution containing Zn<sup>2+</sup>, Mn<sup>2+</sup>, and S<sup>2–</sup> at the desired ratios, the main reactions involve the formation of [Zn(SC(NH<sub>2</sub>)<sub>2</sub>)<sub>2</sub>]<sup>2+</sup> complexes in the solution and the subsequent thermal decomposition of the complex compounds leads to the formation of ZnS:Mn<sup>2+</sup> in an aerosol reactor.



\* To whom correspondence should be addressed. E-mail: okuyama@hiroshima-u.ac.jp.

- (1) Shionoya, S.; Yen, W. M. *Phosphor Handbook*; CRC Press: Boca Raton, FL, 1999.
- (2) Bhargava, R. N.; Gallagher, D.; Hong, X.; Nurmikko, A. *Phys. Rev. Lett.* **1994**, 72, 416.
- (3) Gan, L. M.; Liu, B.; Chew, C. H.; Xu, S. J.; Chua, S. J.; Loy, G. L.; Xu, G. Q. *Langmuir* **1997**, 13, 6427.
- (4) Yu, I.; Isobe, T.; Senna, M. J. *Phys. Chem. Solids* **1996**, 57, 373.
- (5) Yang, H.; Wang, Z. C.; Song, L. Z.; Zhao, M. Y.; Chen, Y. M.; Dou, K.; Yu, J. Q.; Wang, L. *Mater. Chem. Phys.* **1997**, 47, 249.
- (6) Schon, S.; Chaichimansour, M.; Park, W.; Yang, T.; Wagner, B. K.; Summers, C. J. *J. Cryst. Growth* **1997**, 175/176, 598.
- (7) Kina, H.; Yamada, Y.; Maruta, Y.; Tamura, Y. *J. Cryst. Growth* **1996**, 169, 33.
- (8) Nyman, M.; Jenkins, K.; Hampden-Smith, M. J.; Kodas, T. T.; Duesler, E. N.; Rheingold, A. L.; Liable-Sands, M. L. *Chem. Mater.* **1998**, 10, 914.

- (9) Messing, G. L.; Zhang, S. C.; Jayanthi, G. V. *J. Am. Ceram. Soc.* **1993**, 76, 2707.
- (10) Xia, B.; Lenggoro, I. W.; Okuyama, K. *Adv. Mater.* **2001**, 13, 1579.
- (11) Falcony, C.; Garcia, M.; Ortiz, A.; Alconso, J. C. *J. Appl. Phys.* **1992**, 72, 1525.
- (12) Yoon, K. H.; Ahn, J. K.; Cho, J. Y. *J. Mater. Sci.* **2001**, 36, 1373.
- (13) Dimitrova, V.; Tate, J. *Thin Solid Films* **2000**, 365, 134.

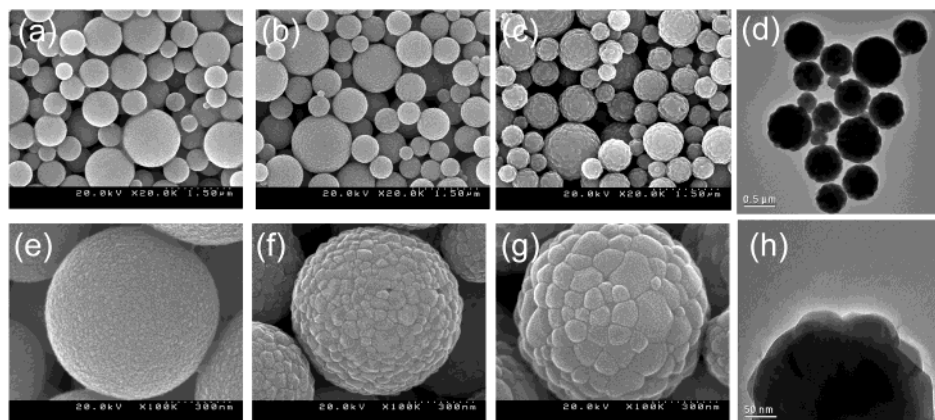


**Figure 1.** ZnS particles synthesized using a nitrate precursor at different temperatures with Mn:Zn = 1:1. (a) 800 °C, (b) 900 °C, (c) 1000 °C; (e), (f), and (g) are high-resolution images (FE-SEM) of (a), (b), and (c) samples, respectively. (d) and (h) are the low- and high-resolution TEM images, respectively, of sample (c). Note: the small bright dots on the particle surfaces are metal formed by sputtering during FE-SEM sample preparation.

$Mn^{2+}$  doping concentration was expressed as a molar ratio based on  $Zn^{2+}$  (Mn:Zn). Under typical conditions, the  $Zn^{2+}$  concentration,  $Mn^{2+}$  doping level, and Tu concentration in a precursor solution were kept at 0.2 mol/L, 1.0 at. %, and 1.0 mol/L, respectively, unless otherwise stated.

The experimental apparatus used in this work was the same as that described in a previous report.<sup>15</sup> The precursor solution was misted by an ultrasonic atomizer (1.7 MHz, NE-U11B, Omron), which generates water droplets about 5  $\mu$ m in diameter. The solution droplets were then carried by a stream of  $N_2$  gas (1.0 L/min) into a tubular ceramic reactor (heating length 1.0 m, inner diameter 13 mm) kept at 400–1000 °C. The residence time of the droplets in the reactor was <5 s. The products were collected in an electrostatic precipitator kept at 150 °C.

Particle size and morphology were observed using a field-emission SEM (Hitachi S-5000) under an acceleration voltage of 20 kV. A field-emission TEM (Hitachi HF-2000) operated at 200 kV was also used to observe the particles. The crystalline phase was determined by an X-ray powder diffraction (XRD) technique (Rint 2200V, Rigaku). The spectrometer (Shimadzu RF-5300PC) includes a powder holder, permitting the photoluminescence of particles to be measured at room temperature. The powder samples were inserted in the holder made from a cylinder of aluminum with a radius of 2.25 mm and height of 1.50 mm. A xenon lamp was used for the excitation of particles in the UV region. When the powders were loaded into the cell, identical conditions were used each time to eliminate any discrepancy in sample preparation conditions.

## Results

**1. Synthesis and Structure.** ZnS: $Mn^{2+}$  particles were produced in the temperature range of 400–1000 °C. The products synthesized from the nitrate precursors are yellow and the color becomes more faint with increasing synthesis temperature, that is, from a deep yellow at 400 and 600 °C to yellow at 800 °C and nearly white at 1000 °C. The samples formed from the nitrate precursors are referred to here as nitrate products. In the 400–800 °C range, the particle did not show any notable changes in morphology. Figure 1 shows the SEM images of the ZnS: $Mn^{2+}$  powders at 1.0 at. % doping formed at 800–1000 °C. At 800 °C, the particles have smooth surfaces, which is similar to products formed

**Table 1. Crystalline Sizes of ZnS: $Mn^{2+}$  Products (1% Mn Doping) Synthesized at Various Temperatures**

temperature (°C)	400	500	600	700	800	900	1000
crystalline size (nm)	<3	<3	<3	4.4	14.4	37.6	73.2

at lower temperatures. At temperatures above 900 °C, particle surfaces became rough and this became more pronounced at 1000 °C. This arises from the rapid crystal growth at 800–1000 °C. Typical TEM images (Figure 1d,h) show that the particles have dense microstructures. Nonagglomerated particles formed from nitrate and acetate precursors are shown in Figure 1. Table 1 shows the crystalline sizes of the nitrate products synthesized at the given temperatures, which were obtained from XRD patterns and the Scherrer's equation. It is obvious that the crystals grow rapidly at temperatures above 800 °C, while at 700 °C and below the crystalline sizes are very small. All nitrate products appear spherical and have dense or nearly dense microstructures. A small amount of large particles have concave surfaces.

We also synthesized ZnS: $Mn^{2+}$  particles at various  $Mn^{2+}$  doping levels (0, 0.125, 0.25, 0.5, 1.0, 2.0, 4.0, and 8.0%), and the particles showed similar morphologies. We changed the  $Zn(NO_3)_2$  concentration (0.1, 0.2, 0.4, and 0.6 mol/L) (and  $Mn^{2+}$  concentration as well, so as to keep the same doping level) while fixing the thiourea concentration at 1.0 mol/L. Larger particles were produced with increasing  $Zn(NO_3)_2$  concentration but maintained a spherical shape. The amount of concave particles also increased with zinc concentration, especially at 0.6 mol/L  $Zn(NO_3)_2$ . This may result from the decreased stability of  $[(Zn,Mn)(SC(NH_2)_2)_2]^{2+}$  complexes ions in the precursor solution at decreasing Tu/Zn ratios.

Figure 2 illustrates ZnS: $Mn^{2+}$  particles synthesized from the chloride and the acetate precursors at 1.0 at. % doping at 800 °C. The particle morphologies of these two products are remarkably different. Significantly different from the nitrate products, the chloride products are characterized by their quite rough surfaces and the presence of connection necks between the particles. The acetate products, on the other hand, appear to be similar to the nitrate products in terms of their particle morphology. It is obvious that all three types of products have spherical shapes and dense structures (confirmed by transition electron microscopy (TEM) with mean

(14) Lenggoro, I. W.; Okuyama, K.; de la Mora, J. F.; Tohge, N. *J. Aerosol Sci.* **2000**, *31*, 121.

(15) Xia, B.; Lenggoro, I. W.; Okuyama, K. *J. Mater. Res.* **2000**, *15*, 2157.

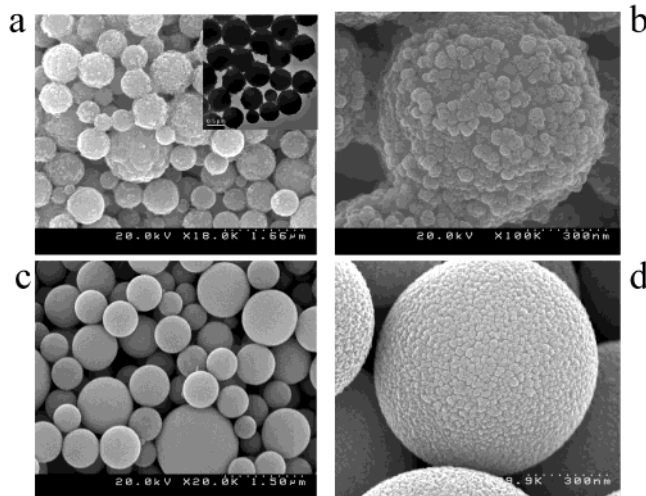


**Figure 2.** ZnS:Mn particles synthesized from (a,b) chloride and (c,d) acetate. The inset of (a) shows a TEM image.

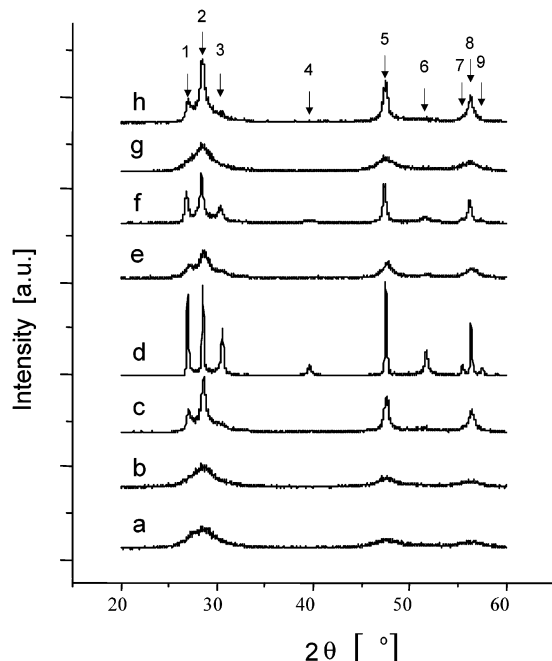


**Figure 3.** XRD patterns of ZnS:Mn products synthesized from (a–d) nitrate products at 400, 600, 800, and 1000 °C; (e,f) chloride products at 600 and 800 °C, respectively; (g,h) acetate products at 600 and 800 °C, respectively. 1, hex(100); 2, cub(111)/hex(002); 3, hex(101); 4, hex(102); 5, cub(220)/hex(110); 6, hex(103); 7, hex(200); 8, cub(311)/hex(112); 9, hex(201).

sizes of around 0.5  $\mu\text{m}$ ). From the SEM images shown above, the chloride product shows the largest crystalline size of the three types of products synthesized using the same experimental conditions except for the anionic sources used. This is also evident in the XRD patterns shown in Figure 3.

Bulk ZnS:Mn<sup>2+</sup> powder phosphors are conventionally produced by firing ZnS powders at 900–1200 °C. The products fired below 1000 °C are a cubic phase (zinc blende), and a hexagonal (wurtzite) is produced at temperatures above 1000 °C.<sup>1</sup> Figure 3 shows the XRD patterns of the products. For the nitrate products, the samples synthesized at 400 and 600 °C show cubic phases; it is difficult to determine the presence/absence of the hexagonal phase due to the broadened lines. The hexagonal phase predominates when the temperature

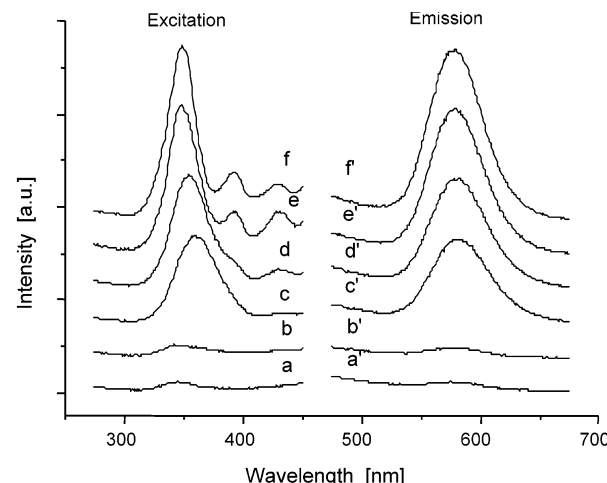


**Figure 4.** Excitation and emission spectra of nitrate products: (a,a') 400 °C; (b,b') 700 °C; (c,c') 800 °C; (d,d') 850 °C; (e,e') 900 °C; (f,f') 1000 °C.

**Table 2. Excitation and Emission Bands of Nitrate Products Synthesized at Various Temperatures**

temperature (°C)	excitation (nm)	intensity (a.u.)	emission (nm)	intensity (a.u.)
400	346	4.5	577	4.2
600	346	4.6	577	4.3
700	346	5.2	577	4.5
800	359	37	581	36
850	354	49	580	47
900	349	63	578	62
1000	349	66	578	58

reaches 800 °C. The chloride products show the presence of hexagonal phase even at 600 °C. The acetate product formed at 800 °C shows the presence of hexagonal phase, but the (101) plane is not well-developed. We also found that increasing the Tu concentration in the solution slightly enhances the crystallinity of the products in all cases.

**2. Optical Property.** Figure 4 shows the excitation and emission spectra of the nitrate products synthesized at 400–1000 °C. The peaks and intensities of the excitation and emission bands are shown in Table 2. The doping level was 1.0 at. % for all samples. In the excitation spectra (emission wavelength  $\lambda = 580$  nm), the samples synthesized at 400–700 °C do not show any significant photoluminescence. Since the intensities are at the same level as the zero doping product (ZnS), this indicates that Mn<sup>2+</sup> is not activated in these products. The products formed at 800 °C have significant photoluminescence (excitation 359 nm), which is a characteristic emission of ZnS:Mn<sup>2+</sup> and can be attributed to a  $4\text{T}_1 \rightarrow 6\text{A}_1$  transition of Mn<sup>2+</sup> ion in  $T_d$  symmetry.<sup>3,4</sup> The band then becomes blue-shifted and the intensity increases from 800 to 850 °C and further to 900 °C. The band does not continue to shift and the intensity increases only marginally from 900 to 1000 °C. The emission bands are centered at 580 nm.

From the photoluminescence intensities shown in Table 2 and the XRD patterns in Figure 3, the hexagonal phase, instead of the cubic phase, is luminescence-active. Nanometer ZnS:Mn<sup>2+</sup> phosphors have been shown to show a quantum size effect, that is, the photoluminescence shifts to blue and the intensity increases with decreasing crystalline size when the size is sufficiently small.<sup>3–5</sup> The ZnS:Mn<sup>2+</sup> nanocrystals

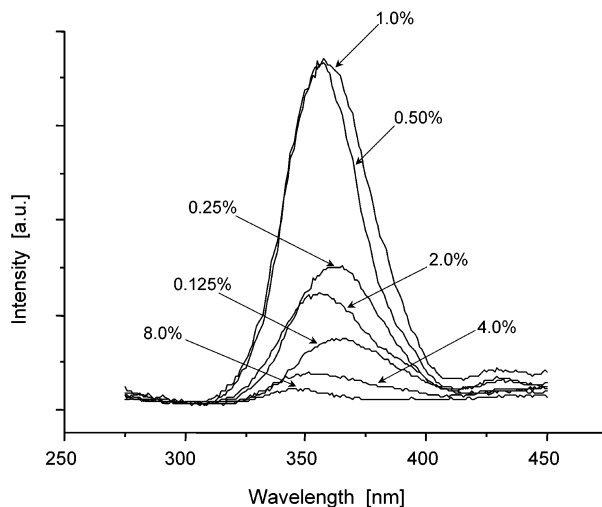


**Figure 5.** Excitation spectra of nitrate products synthesized at 800 °C using various Mn<sup>2+</sup> doping levels.

**Table 3. Effects of Mn<sup>2+</sup> Doping Levels on Excitation Bands**

Mn <sup>2+</sup> doping (at. %)	wavelength (nm)	intensity (a.u.)
0.125	364	15
0.25	362	30
0.50	358	73.8
1.0	357	73.5
2.0	356	24
4.0	351	7.7
8.0	348	4.2

formed in this work had mean sizes from <3 to >70 nm. The results show that the higher the crystallinity of the hexagonal phase, the higher the photoemitting efficiency, which is different from the quantum size effect.

Figure 5 and Table 3 show the effects of the Mn<sup>2+</sup> doping level (between 0.125 and 8.0% in atomic ratio) on the precursor. The excitation intensity becomes stronger with increasing doping level from 0.125 to 0.50% and does not change greatly at 1.0%. Thus, the optimum Mn<sup>2+</sup> doping concentration is 0.5–1.0% in atomic ratio. The intensity then decreases with further doping, showing the concentration quenching effect. Aerosol decomposition derived ZnS:Mn<sup>2+</sup> thin films have been reported to show the same effect,<sup>11,12</sup> and a much higher doping level (7.0 at. %) was observed.<sup>12</sup>

The influence of [Tu] and [Zn<sup>2+</sup>] concentrations was also investigated. The products were synthesized from nitrate precursors at 800 °C. With increasing [Tu] concentration in the range 0.4–1.0 mol/L with the other conditions fixed, the intensities of the excitation/emission bands increased and the excitation bands shifted to blue (from 375 nm at 0.4 mol/L to 359 nm at 1.0 mol/L). With increasing Zn concentration from 0.2 to 0.6 M, with the other conditions fixed, the excitation bands become red-shifted and the emission intensities decreased. We also observed that when the Zn concentration decreased to 0.1 mol/L, the photoluminescence intensity dropped significantly and the color of the powder turned to brown, which was different from other yellow(ish) products.

The effects of different types of precursors (cationic sources) are shown in Figure 6. The excitation bands are blue-shifted in the sequence of nitrate, chloride, and acetate products, while the band strengths decrease in

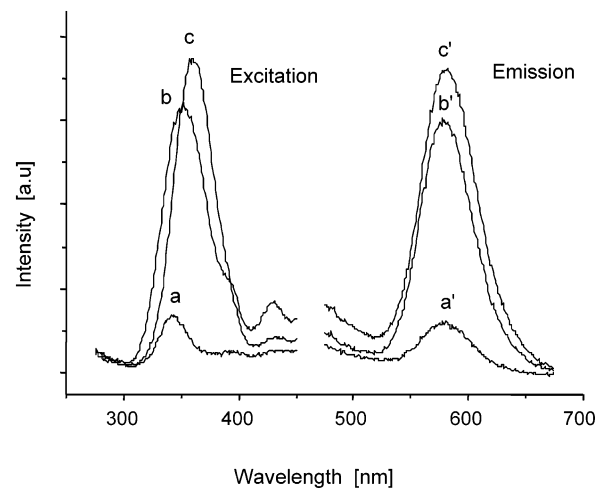


**Figure 6.** Excitation and emission bands of nitrate, chloride, and acetate products synthesized at 800 °C at 1.0% Mn doping. (a,a') acetate products; (b,b') chloride products; (c,c') nitrate products.

the same order. The nitrate product has the strongest photoluminescence.

## Discussion

Thiourea (Tu) is a good source for forming metal sulfides by aerosol decomposition and plays several important roles in the synthesis process. First, it forms stable complexes with Zn<sup>2+</sup> and Mn<sup>2+</sup>, which are easily soluble in water. This is responsible for the formation of dense and spherical particles. Second, it prevents the metal sulfide from being oxidized in the reactor, where water vapor functions as an oxidizing agent. Therefore, an external protective gas, for example, H<sub>2</sub>S, is not necessary for the synthesis. For example, we found that when the ratio of Tu/Zn is down to 1:1 ([Tu] = 0.2 mol/L, stoichiometric ratio) in the solution, minor hexagonal ZnO (Zincite) coexists with the major ZnS phase in the product synthesized at 800 °C. Third, Tu is readily decomposed to gaseous byproducts that are easily removed from product. Furthermore, we also found that increasing the Tu concentration in the solution leads to a slight enhancement in product crystallinity. An increase in crystalline size with increasing S<sup>2-</sup>/Zn<sup>2+</sup> ratio was also observed in a recent study involving colloidal synthesis.<sup>16</sup>

In spray pyrolysis, after precursor decomposition, since the product particle sizes are at the micrometer level, that is, much larger than nanoparticles, they do not sinter or coalesce to agglomerate in the reactor under the typical synthesis conditions (especially, temperature and residence time). In addition, the forces/interactions among the micrometer particles are usually considered weak compared to those of nanosized particles where strong interactions exist. Therefore, aerosol decomposition derived particles are usually considered to be nonagglomerated under typical conditions.<sup>9</sup> This work indicated that the same situation holds for the nitrate and the acetate products. The chloride products, however, show an unexpected existence of agglomeration (Figure 2). This implies that some compound(s) are

present in the reactor (e.g., chloride salts) having low melting point(s) that formed in the particles, which melts at the synthesis temperatures. (Note: ZnS melts at much higher temperature, 1700 °C.) Thus, when two or more particles collide in the gas phase in the reactor, it is likely that they would agglomerate. The formation of melted compound(s) may also be a possible reason for why chloride products have the largest degree of crystallinity among the three products formed under the same conditions because the melt can act as a solvent for crystals to grow up rapidly.<sup>10,17</sup> The melt(s) may be removed (or partly removed) from or reside in the particles after the synthesis process, depending on experimental conditions.

It is well-known that Mn<sup>2+</sup> can substitute for Zn<sup>2+</sup> ions in the ZnS crystal lattice because of their close ionic radii (0.80 and 0.83 Å for Mn<sup>2+</sup> and Zn<sup>2+</sup>, respectively). The photoluminescence emission band at around 580 nm (yellowish orange) is a characteristic emission of Mn<sup>2+</sup> ions in ZnS crystals, which can be attributed to a <sup>4</sup>T<sub>1</sub> (excited) → <sup>6</sup>A<sub>1</sub> (ground) transition of Mn<sup>2+</sup> ion in *T*<sub>d</sub> symmetry.<sup>3,4</sup> The emission takes place via energy transfer from the excited state of the ZnS host lattice to the *d* electrons of Mn<sup>2+</sup>.

The homogeneous distribution of Mn<sup>2+</sup> ions in a ZnS crystal lattice is very important for highly efficient luminescence.<sup>3,4,18,19</sup> For the inhomogeneous distribution of Mn<sup>2+</sup> ions, local Mn<sup>2+</sup>–Mn<sup>2+</sup> pairs or clusters are formed in the ZnS crystals, which interact and lead to nonradiative relaxation under excitation.<sup>19,20</sup> This results in a low luminescence efficiency. During the AD process, ZnS forms the main phase while Mn<sup>2+</sup> is present as an impurity and can gradually be incorporated into the ZnS crystal lattice, depending on process conditions. With an increase in process temperature, Mn<sup>2+</sup> can effectively diffuse into the ZnS lattice, forming a homogeneous solid solution throughout the crystals.<sup>4</sup> Higher temperatures also promote a higher degree of crystallinity, thus eliminating crystal defects. Therefore, luminance usually increases with process temperature in a suitable temperature range. At 700 °C and below, the products do not show luminance because the crystallinity is poor (see Figure 3) and Mn<sup>2+</sup> has not been effectively incorporated into the ZnS crystal lattices, probably existing near the ZnS crystal surfaces. The crystals grow rapidly at 800 °C, implying a significant enhancement in the movement of Mn<sup>2+</sup> and Zn<sup>2+</sup> ions and rearrangements both on the surface and in the bulk of ZnS. This is beneficial to the spatial isolation or homogenization of Mn<sup>2+</sup> ions as well as the elimination of crystal defects. As a result, photoluminescence increases in the temperature range 800–850 °C and further to 900 °C. From 900 to 1000 °C, luminance is only marginally increased. This suggests that, at 900 °C, Mn<sup>2+</sup> ions are nearly homogeneously distributed in the ZnS crystal lattices and a further increase in temperature makes little contribution to the luminescence efficiency. The red shift of the excitation bands

with decreasing temperatures can be attributed to local Mn<sup>2+</sup>–Mn<sup>2+</sup> interactions due to high concentration present.<sup>1</sup> Besides ZnS:Mn<sup>2+</sup> phosphor, other Mn<sup>2+</sup>-activated phosphors, for example, Mg<sub>1-x</sub>Al<sub>2</sub>O<sub>4-x</sub>:Mn<sup>2+</sup> and Mg<sub>1-x</sub>Ga<sub>2</sub>O<sub>4-x</sub>:Mn<sup>2+</sup>, also show luminescent sensitivity to Mn<sup>2+</sup> distribution in host lattices.<sup>21</sup>

This work also demonstrated the influence of [Tu] and [Zn<sup>2+</sup>] concentrations. With increasing Tu concentration with all other conditions fixed, the intensities of the excitation and emission bands increased and the excitation bands shifted toward blue, as shown above. This may be attributed to the increasing [Tu] concentration; the incorporation of [Mn<sup>2+</sup>] into the ZnS crystal lattice is promoted (i.e., the Mn<sup>2+</sup> distribution is homogenized) due to the increase in product crystallinity, although the mechanism for this is unclear. When the [Zn<sup>2+</sup>] concentration is increased from 0.2 to 0.6 mol/L while the other conditions are fixed, the Tu/Zn<sup>2+</sup> ratio decreases from 1:1 to 1:3, and as a result the emission intensities decrease.

An improvement in the quantum size effect of a ZnS:Mn<sup>2+</sup> phosphor, that is, the luminescence efficiency with the blue-shift band in nanocrystals, has frequently been observed in crystals with a mean size mostly below 5 nm.<sup>2–4,16</sup> In such low-dimensional crystals, efficient energy transfer from the excited state of the ZnS host lattice to the *d* electrons of the Mn<sup>2+</sup> dopant and wave function mixing between *d* electrons of Mn<sup>2+</sup> and *s* electrons and *p* holes of the ZnS nanocrystals explain this size effect. It is interesting to note that, in this work, the crystalline size was as small as <3 nm, but a size effect was not observed. We conclude that this phenomenon may also be related to the Mn<sup>2+</sup> distribution in the ZnS lattice. At very small crystalline sizes (<5 nm for the products formed at ≤700 °C) because Mn<sup>2+</sup> is not incorporated well into the ZnS lattice due to the low temperatures, luminescent efficiency is very low. At ≥800 °C, Mn<sup>2+</sup> photoemission is largely improved due to spatially isolated Mn<sup>2+</sup> ions in the ZnS lattice, but the crystal sizes become too large (>10 nm) to permit an observation of a quantum size effect.

Figure 5 shows the concentration quenching effect. Concentration quenching has been widely observed,<sup>19,22</sup> although a few exceptions have been noted.<sup>23</sup> The existence of optimum Mn<sup>2+</sup> doping concentration has been attributed to the presence and interaction of Mn<sup>2+</sup>–Mn<sup>2+</sup> ion pairs or clusters at increasing Mn<sup>2+</sup> concentrations.<sup>19</sup> The process involves resonant transfer of electronic excitation energy from one activator ion (Mn<sup>2+</sup>) to another and, after a number of energy transfer steps, to a quenching site (e.g., a defect).<sup>22</sup>

Figure 6 shows the effects of different precursors on luminescence properties, in addition to the effects on particle morphology and crystalline phase as shown in Figures 1–3. In an aerosol decomposition process, ligands are precipitated with the cations during droplet drying followed by thermal decomposition at higher temperatures and can then either reside in solid products as impurities or form gaseous products that can be removed, depending on process conditions. For

(17) Gopalan, S.; Virkar, A. V. *J. Electrochem. Soc.* **1993**, *140*, 1060.  
(18) Hunter, A.; Kitai, A. H. *J. Appl. Phys.* **1987**, *62*, 4244.

(19) Yu, I.; Senna, M. *Appl. Phys. Lett.* **1995**, *66*, 23.

(20) Bessergenev, V. G.; Belyi, V. I.; Rastorguev, A. A.; Ivanova, E. N.; Kovalevskaya, Yu. A.; Larionov, V. G.; Zemskova, S. M.; Chirichenko, V. N.; Nadolinnyi, V. A.; Gromilov, S. A. *Thin Solid Films* **1996**, *279*, 135.

(21) Mohler, R. L.; White, W. B. *Mater. Res. Bull.* **1994**, *29*, 1109.  
(22) Blasse, G.; Grabmaier, B. C. *Luminescent Materials*; Springer-Verlag: Berlin, 1994.

(23) Bol, A. A.; Meijerink A. *J. Phys. Chem. B* **2001**, *105*, 10197.

nitrate precursors, since they usually decompose to  $\text{NO}_x$  gases at relatively low temperatures, for example,  $<400$  °C, the products in our work are free of ligand contamination and show a high degree of luminescence. However, for the acetate and chloride precursors, carbon or chlorine may be left in the particles, especially when a sufficiently high temperature is used. For example, the powder colors are deep yellow and brownish for the chloride and the acetate products, respectively, when formed at 800 °C, which are slightly different from the yellow nitrate products formed under the same conditions. Although elemental analysis indicated the presence of only a small amount of chlorine and carbon impurities, at levels of  $10^{-3}$  to  $10^{-2}$  by weight in the 800 °C products, they may cause a significant influence on the photoluminescence properties since they tend to concentrate near the surface of the ZnS crystals due to their large ionic size or low solubility in the crystals. Their existence may decrease the energy-transfer efficiency from the ZnS host lattice to  $\text{Mn}^{2+}$  or/and they may interact with  $\text{Mn}^{2+}$  ions and act as quenching sites. The interaction between impurities and ZnS: $\text{Mn}^{2+}$  may also alter the excitation band or band gap (shown in Figure 6), although the mechanism for this is not clear. The precursor effects shown here are different from some solution-based ZnS: $\text{Mn}^{2+}$  phosphors, where no precursor effects were observed because all the ligands were washed away after precipitation.<sup>16</sup>

### Conclusion

ZnS: $\text{Mn}^{2+}$  phosphor particles were synthesized for the first time using aerosol decomposition from nitrate, chloride, and acetate precursors and Tu in the temperature range 400–1000 °C. The results show that aerosol decomposition leads to the formation of spherical and dense ZnS: $\text{Mn}^{2+}$  particles with micrometer/submicrometer sizes, homogeneous morphologies, and nonagglom-

eration, which consist of nanocrystals ranging from  $<3$  to  $>70$  nm. Different from the nitrate and acetate products, the chloride products have a higher crystallinity and rough surfaces and contain a portion of agglomerated particles. The photoluminescence of the ZnS: $\text{Mn}^{2+}$  particles is strongly dependent on the synthesis conditions. Samples formed at low temperatures (e.g., 400–700 °C) show a cubic symmetry and  $\text{Mn}^{2+}$  is not activated under excitation, while high-temperature ( $\geq 800$  °C) products are present as a hexagonal phase and show a strong orange emission due to the homogenized distribution of  $\text{Mn}^{2+}$  ions in the ZnS crystal lattice. The nitrate product has the strongest emission while the acetate product yields the smallest under the same synthesis conditions. Since the products show strong emission and a unique particle morphology, that is, spherical and dense particles with nonagglomeration, densely compacted products (e.g., the powder compact derived from aerosol decomposition can easily reach as high as around 60% of the theoretic density under pressure)<sup>9</sup> with high emitting efficiencies could be readily fabricated into devices, for use in phosphor applications.

**Acknowledgment.** We thank the Japan Society for the Promotion of Sciences (JSPS) and the Ministry of Education, Culture, Sports, Science and Technology of Japan for a postdoctoral fellowship (B.X.), Grant-in-Aid for Exploratory Research (K.O. and I.W.L.), and Grant-in-Aid for Encouragement of Young Scientists (I.W.L.). This work was also supported in part by the New Energy and Industrial Technology Development Organization (NEDO)'s "Nanotechnology Materials Program—Nanotechnology Particle Project" based on funds provided by the Ministry of Economy, Trade and Industry, Japan (METI).

CM020409I